INTERFACE

royalsocietypublishing.org/journal/rsif

CC BY

Research

Cite this article: John RS, Fatoyinbo HO, Hayman DTS. 2024 Modelling Lassa virus dynamics in West African *Mastomys natalensis* and the impact of human activities. *J. R. Soc. Interface* **21**: 20240106.
https://doi.org/10.1098/rsif.2024.0106

Received: 12 February 2024
Accepted: 4 June 2024

Subject Category:
Life Sciences–Mathematics interface

Subject Areas:
biomathematics, ecosystem

Keywords:
Lassa fever, time-average basic reproductive number, $\widetilde{\mathcal{R}}_p$, climate change, land use change

Author for correspondence:
David T. S. Hayman
e-mail: d.t.s.hayman@massey.ac.nz

†All authors contributed equally to the study.

‡Present address: Auckland University of Technology, Auckland, New Zealand.

Electronic supplementary material is available online at https://doi.org/10.6084/m9.figshare.c.7355003.

THE ROYAL SOCIETY PUBLISHING

Downloaded from https://royalsocietypublishing.org/ on 31 July 2024

Modelling Lassa virus dynamics in West African *Mastomys natalensis* and the impact of human activities

Reju Sam John†, Hammed Olawale Fatoyinbo†,‡ and David T. S. Hayman†

Massey University, Private Bag, 11 222, Palmerston North 4442, New Zealand

RSJ, 0000-0002-5024-3700; HOF, 0000-0002-6036-2957; DTSH, 0000-0003-0087-3015

Lassa fever is a West African rodent-borne viral haemorrhagic fever that kills thousands of people a year, with 100 000 to 300 000 people a year probably infected by Lassa virus (LASV). The main reservoir of LASV is the Natal multimammate mouse, *Mastomys natalensis*. There is reported asynchrony between peak infection in the rodent population and peak Lassa fever risk among people, probably owing to differing seasonal contact rates. Here, we developed a susceptible-infected-recovered (*SIR*)-based model of LASV dynamics in its rodent host, *M. natalensis*, with a persistently infected class and seasonal birthing to test the impact of changes to seasonal birthing in the future owing to climate and land use change. Our simulations suggest shifting rodent birthing timing and synchrony will alter the peak of viral prevalence, changing risk to people, with viral dynamics mainly stable in adults and varying in the young, but with more infected individuals. We calculate the time-average basic reproductive number, $\widetilde{\mathcal{R}}_p$, for this infectious disease system with periodic changes to population sizes owing to birthing using a time-average method and with a sensitivity analysis show four key parameters: carrying capacity, adult mortality, the transmission parameter among adults and additional disease-induced mortality impact the maintenance of LASV in *M. natalensis* most, with carrying capacity and adult mortality potentially changeable owing to human activities and interventions.

1. Introduction

Lassa fever is a viral haemorrhagic fever (VHF) caused by Lassa virus (LASV, species *Mammarenavirus lassaense*). LASV is endemic in West Africa. Approximately 100 000 to 300 000 people may be infected annually, with a fatality rate of 1–2% of cases, though reported case fatality rates can be much higher [1,2]. The main reservoir of LASV, the species in which the virus persists at the population level, is the Natal multimammate mouse, *Mastomys natalensis*, though numerous species have contact with LASV and may become infected [1,3]. *Mastomys natalensis* is a rodent species that is not only infected with LASV, but lives in villages and agricultural habitats throughout West Africa [4,5]. Humans probably become infected through the ingestion of food or water contaminated with LASV-positive droppings and urine, the inhalation of aerosolized virus particles or sometimes the direct consumption of LASV infected mice [4,6]. Human-to-human transmission is rare, though reported from households and hospitals, so the main source of infection in people is zoonotic (animal to human) [7–9]. The first-in-human phase 1 vaccine trial results have been recently published and are promising [10], but there is currently no licensed vaccine or effective treatment, and, given the high case fatality and evidence of human-to-human transmission, the World Health Organization includes LASV as a priority pathogen of epidemic potential.

© 2024 The Authors. Published by the Royal Society under the terms of the Creative Commons Attribution License http://creativecommons.org/licenses/by/4.0/, which permits unrestricted use, provided the original author and source are credited.

Downloaded from https://royalsocietypublishing.org/ on 31 July 2024

Table 1. Parameters and variables.

term	description	values	units	source/comments
$\nu(t)$	birth rate	$\alpha_0 + ke^{(-s\cos^2(\pi t-\varphi))}$	per female day^{-1}	our calculation
t	time	1 to 365	day	NA
α_0	baseline birth rate	2.77/30	per female day^{-1}	our calculation
k	scaling factor	4.51/30	day^{-1}	our calculation
s	bandwidth (time span of the birth pulse)	31.021	days	our calculation
φ	phase shift	0.58	radians	our calculation
ρ	proportion of young born infected	0.1		[14]
μ_j	death rate of juvenile	0.013	per capita day^{-1}	[32]
μ_a	death rate of adult	0.02	per capita day^{-1}	[33]
θ	additional disease-induced mortality	1.05		[34]
β_{jj}	juvenile-to-juvenile transmission rate	1.45e−3	per capita day^{-1}	[35]
β_{ja}	juvenile-to-adult transmission rate	1.45e−3	per capita day^{-1}	[35]
β_{aa}	adult-to-adult transmission rate	1.45e−3	per capita day^{-1}	[35]
β_c	transmission rate from chronic class	1.45e−3/2	per capita day^{-1}	our assumption; $\beta_{xx}/2$
γ_j	recovery rate of juvenile rodents	0.0457	day^{-1}	[35]
γ_a	recovery rate of adult rodents	0.0457	day^{-1}	[35]
τ_j	ageing rate of juvenile to adult rodents	0.0166	day^{-1}	[36]
K	carrying capacity	1000		

The natural LASV host, *M. natalensis* is distributed all over sub-Saharan Africa, where it also hosts other arenaviruses [11], yet while suitable habitat exists that might allow the ecological opportunity for viral spread among regions, different sub-taxa among *M. natalensis* have different ranges, and these support intrinsic barriers among hosts, preventing infection with different viruses, thus explaining why human cases of LASV are limited to West Africa [12].

The risk of LASV infection is seasonal [4,13]. However, there has been a reported disconnect (asynchrony) between the dynamics of hosts [14] and infection in hosts [4] and human risk (though possible exceptions exist [15], supported by some recent modelling work [16]). Most human LASV infections occur in the dry season (probably owing to contact), yet viral prevalence and rodent breeding are higher in the rainy season [4]. Prevention of LASV infection is currently effectively limited to hygiene and rodent control. However, recent studies have shown some mouse control approaches might alter the dynamics and even lead to increases in host infection, and therefore human risk, following population recovery [17], a phenomenon also possibly observed after efforts to cull bats infected with VHF-causing marburgviruses [18]. Together, these findings suggest rodent behaviours and their responses to the environment may play a key role in determining human infection and disease risk [4,14,16]. This risk might change owing to land use and climate change, along with human population growth in West Africa [19,20].

Few mathematical models have examined the seasonal dynamics of LASV and incorporated rodent dynamics, with recent models aiming to fit spillover models to data and understand changes in risk, including with seasonal variation and how rodent control might impact the risk of LASV infection among people [13,16,21–23]. The historic gap is partly probably owing to the gaps in knowledge and data available on *M. natalensis* populations and LASV in West Africa, despite the obvious public health impacts [1] and the species importance as a crop pest [24–27]. However, this gap needs filling. *Mastomys natalensis* is generalist species, feeding on various available resources depending on the season and the habitat [25,28], including crops such as maize [29], causing population densities to coincide with resource availability [27]. West Africa and Africa in general are going through substantial land use change, potentially changing habitats and disease risk [30] and will be impacted by climate change [31], all impacting resource availability for *M. natalensis* and contact rates between them and people [19].

Here, we investigate the seasonal dynamics of LASV in a model *M. natalensis* population to further help understand how the host population dynamics might affect viral persistence in the population, its dynamics, and how changing host dynamics, such as in response to land use or climate change, might impact infection dynamics.

2. Methods

We follow recent arenavirus susceptible–infected–recovered (*SIR*) models in *M. natalensis* [23,32] based on field observations and experimental infection data, occasionally using other rodent-mammarenavirus data if *M. natalensis*-LASV data are not available (table 1). The *SIR* model structure incorporates demography (births; ν and deaths; μ). Field and experimental data

Downloaded from https://royalsocietypublishing.org/ on 31 July 2024

suggest some individuals can be chronically (persistently) infected and infectious, so we include a chronic class (C) [23,37,38], and that while most infection is horizontal [39], there is evidence of vertical transmission (or pseudo-vertical, to suckling young) in approximately 10% of young (the viral prevalence in pregnant females [14]), with neonatally infected animals acquiring chronic infection [14,40,41]. Therefore, we include age structure with adult ($_a$) and juvenile classes ($_j$). As all neonatal *M. natalensis* infected with LASV in an experimental study became chronically infected with simultaneous development of antibodies [40], and the evidence of vertical transmission in approximately 10% of young matches the viral prevalence in pregnant females [14], we assume all young born to infected mothers become chronically infected, leading to a different model structure to [23]. While the impact of infection on *M. natalensis* is not obvious [37], long-term studies suggest there may be an additional disease-induced mortality (approximately 5%) [34], which we include as θ, i.e. $\theta \times \mu X = 1.05 \times \mu X$. Further, following [42] whose work supports LASV transmission being density-dependent transmission, we model transmission as density- and not frequency-dependent transmission, or a mixture of the two [43]. Unlike [23] we do not include maternally derived antibodies or an exposed class and discuss these in the §4. The full *SICR* model is shown in figure 1 and equation (2.1).

$$\begin{aligned}
\frac{dS_j}{dt} &= \nu(t)(S_a + R_a + (1-\rho)(I_a + C_a)) - (\beta_{ja}I_a + \beta_{jj}I_j + \beta_c(C_j + C_a))S_j - \tau_j S_j - \mu_j S_j\left(\frac{N}{K}\right)\\
\frac{dI_j}{dt} &= (\beta_{ja}I_a + \beta_{jj}I_j + \beta_c(C_j + C_a))S_j - \tau_j I_j - \gamma_j I_j - \theta\mu_j I_j\left(\frac{N}{K}\right)\\
\frac{dC_j}{dt} &= \nu(t)(\rho(I_a + C_a)) - \tau_j C_j - \theta\mu_j C_j\left(\frac{N}{K}\right)\\
\frac{dR_j}{dt} &= \gamma_j I_j - \tau_j R_j - \mu_j R_j\left(\frac{N}{K}\right)\\
\frac{dS_a}{dt} &= \tau_j S_j - (\beta_{aa}I_a + \beta_{ja}I_j + \beta_c(C_a + C_j))S_a - \mu_a S_a\left(\frac{N}{K}\right)\\
\frac{dI_a}{dt} &= \tau_j I_j + (\beta_{aa}I_a + \beta_{ja}I_j + \beta_c(C_a + C_j))S_a - \gamma_a I_a - \theta\mu_a I_a\left(\frac{N}{K}\right)\\
\frac{dC_a}{dt} &= \tau_j C_j - \theta\mu_a C_a\left(\frac{N}{K}\right)\\
\frac{dR_a}{dt} &= \gamma_a I_a + \tau_j R_j - \mu_a R_a\left(\frac{N}{K}\right).
\end{aligned} \tag{2.1}$$

The parameters are summarized in the table 1.

We have employed a carrying capacity (a constant K) approach, which is widely used in ecology [44], to control the unrealistic exponential growth of rodents in each compartment of our model, because of *M. natalenis*'s high intrinsic population growth rate [24,26,27]. Carrying capacity is the maximum population size that an environment can support indefinitely, i.e. the largest number of organisms that can live in a certain place without causing environmental issues such as the exhaustion of available food. The equation

$$N_t = \frac{K}{1 + e^{a - rt}}$$

represents how a population grows over time. This is known as the integral form. The equation

$$\frac{dN}{dt} = rN\left(1 - \frac{N}{K}\right)$$

explains how a population changes over time. This is called the differential form. In these equations, N stands for the number of organisms, r is the rate at which the population grows when there is no competition for resources, t is time and a is a constant of integration defining the position of the curve relative to the origin. In the second equation, the part inside the brackets indicates the potential for growth. When the population is small, this value is close to 1, leading to rapid growth. As the population approaches the carrying capacity K, this value decreases towards 0, causing growth to slow down. When the population reaches K, growth stops because the unused growth potential becomes 0. This means there is feedback in the system and that the population ceases to grow when it reaches its carrying capacity.

In our model, we incorporate the variable K to establish an upper limit on the size of the rodent populations in each compartment. This is achieved by the influence of K on the death rate and the size of each compartment (e.g. S, I, C, R), which enhances mathematical, as well as the biological and population, stability. It is important to note that we are implementing the carrying capacity effect on the death rate, which differs from the previous differential equation where the expression within the brackets acted on the growth rate. So in our case, the expression within the brackets takes the form $\frac{N}{K}$, where N represents the total rodent population at time t. Consequently, the death term in our model is expressed as

$$-\mu_y X\left(\frac{N}{K}\right)$$

where $_y$ is the age class $_a$ or $_j$.

The genus *Mastomys* comprises abundant and intensively studied rodents, widespread across sub-Saharan Africa, with *M. natalensis* the best studied [45,46]. However, most data are from regions outside West Africa, which we used to parametrize our model in the absence of the necessary data. Mulungu *et al.* [26] reported that there is a seasonal breeding pattern for *M. natalensis* in Tanzania, East Africa. Although the data from [26] were collected in Tanzania, the multimammate mouse (*M. natalensis*) is a widely distributed species across sub-Saharan Africa, and its reproductive patterns are expected to be

Downloaded from https://royalsocietypublishing.org/ on 31 July 2024

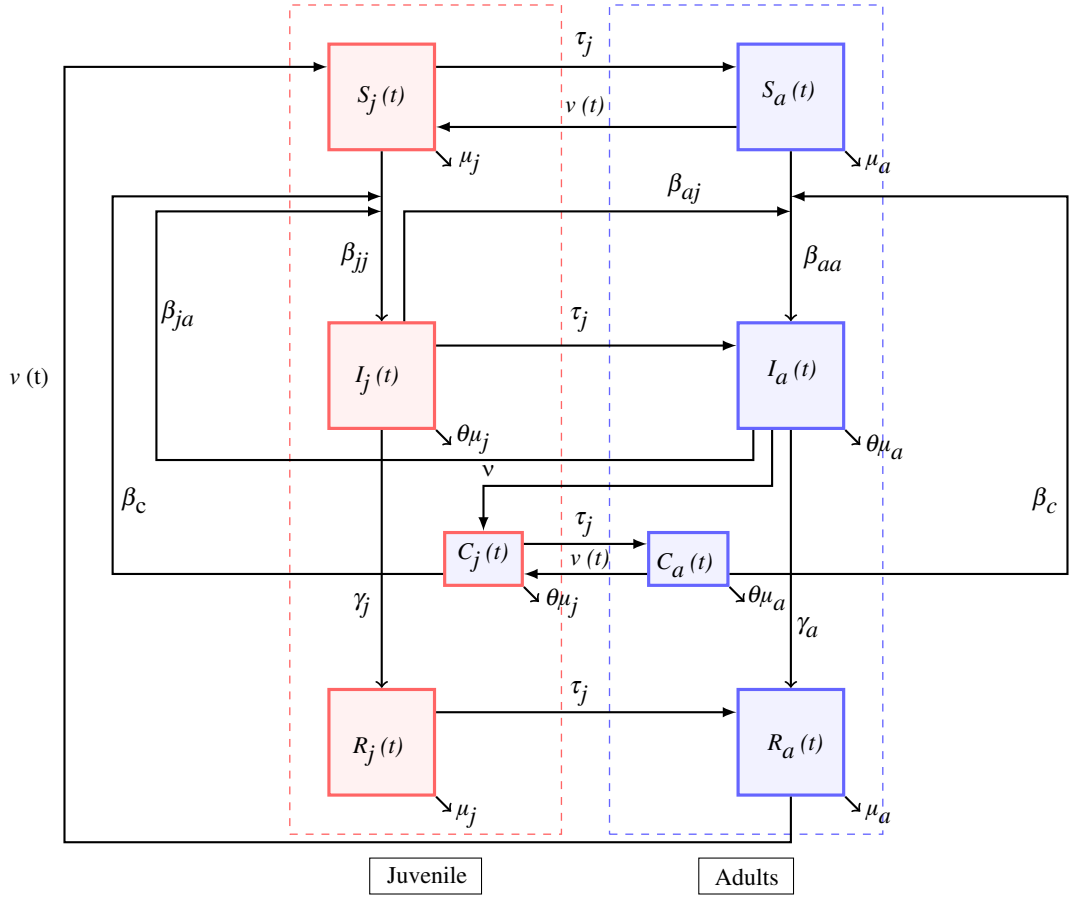

Figure 1. Model structure.

influenced by similar environmental cues and seasonal changes. Therefore, while acknowledging potential regional variations, we extrapolated the observed seasonal breeding pattern to West African populations of *M. natalensis*, which serves as the primary reservoir for LASV transmission. This extrapolation is further supported by previous studies (e.g. [4]) that have documented comparable seasonal fluctuations in the reproductive activity of *M. natalensis* in West African regions, lending credence to the broader applicability of the patterns observed by Mulungu *et al.* [26]. In the Tanzanian study, more juveniles were captured in the months of August and September compared with other months, along with a baseline capture number. We extracted data from [26] with the help of the tool WebPlotDigitizer[1] [47] and fitted the function $\nu(t) = \alpha_0 + ke^{(-s\cos^2(\pi t/12-\varphi))}$ following the approach outlined in [48], except for the baseline birth rate, which is represented by α_0, to the data in [26], as shown in figure 2, where α_0 is the baseline birth rate, k is the birth pulse scaling factor, s is the duration of the birth pulse and φ is the the timing of the peak of the birth pulse.

We need to normalize α_0 and k to obtain the annual per capita birth rate. Safronetz *et al.* [49] reported the reproductive behaviour of West African *M. natalensis*. In their 12 months breeding program of *M. natalensis*, 90 rodents give birth to 1618 pups. So we can say

$$\int_1^{12}\left(\alpha_0 + ke^{(-s\cos^2(\pi t/12-\varphi))}\right)dt = \frac{1618}{90/2} \tag{2.2}$$

assuming an equal number of males and females in the group. Therefore

$$11\alpha_0 + k\int_1^{12}\left(e^{(-s\cos^2(\pi t/12-\varphi))}\right)dt = \frac{1618}{45} \tag{2.3}$$

by substituting the values for s and φ from the fit to the above equation

$$k\int_1^{12}\left(e^{(-31.02\cos^2(\pi t/12-0.59))}\right)dt = \frac{1618}{45} - 11\alpha_0, \tag{2.4}$$

i.e.

$$k \times 1.226 = \frac{1618}{45} - 11\alpha_0 \tag{2.5}$$

[1]A comprehensive user manual can be accessed through the software's GitHub page at https://github.com/automeris-io/WebPlotDigitizer

Downloaded from https://royalsocietypublishing.org/ on 31 July 2024

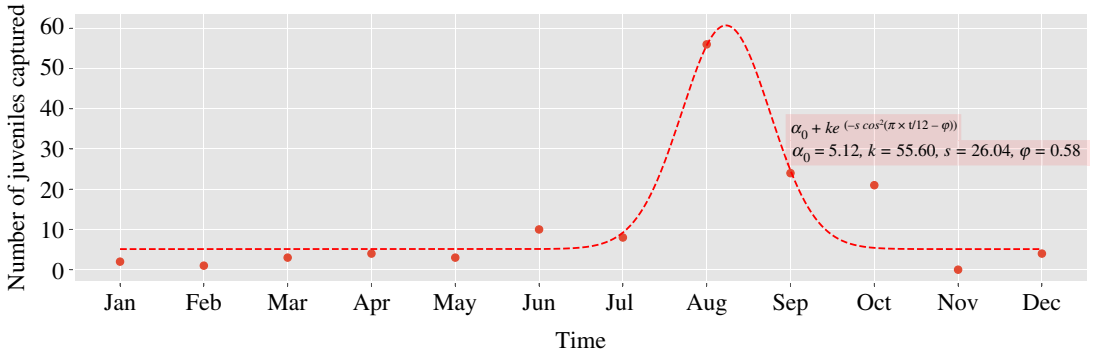

Figure 2. Seasonal breeding pattern of *M. natalensis* overlaid with our fitted birth function curve using data from [26].

or

$$k = \frac{\left(\frac{1618}{45} - 11\alpha_0\right)}{1.226}. \tag{2.6}$$

This is an equation with two unknowns, so we need to fix one before we can continue. On average, a female *M. natalensis* can give birth to nine pups per litter every 3.25 months [49].

So a female *M. natalensis* can produce an average of $\frac{9}{3.25} = 2.775$ offspring per month. Hence α_0, the baseline birth rate per capita per month is 2.775 pups.

Therefore

$$k = \frac{\left(\frac{1618}{45} - 11\frac{9}{3.25}\right)}{1.226} = 4.51. \tag{2.7}$$

Thus, the normalized birth rate is

$$\nu(t) = 2.77 + 4.51e^{(-31.02\cos^2(\pi t/12 - 0.59))} \tag{2.8}$$

shown in figure 2.

Together, this gives us a parametrized LASV-*M. natalensis* S, I, C, R model with which to perform simulation exercises and test the impact of varying scenarios.

2.1. Varying birthing cycles

Mastomys natalensis is a widespread species [45], living in a range of environments, including peridomestically [50], and it is a species that responds to environmental factors such as rainfall and associated food availability [5,24,25,28,29,32]. Given this, human interventions such as land use change [30] and climate change impacts on rainfall [31] will impact *M. natalensis*. Climate and land use change can induce either an expansion (widening) or a contraction (narrowing) of the birth pulse (figure 2) in the *M. natalensis* populations as they impact the availability of resources. To simulate or experiment with such changes, we varied the width of the birth pulse by altering the parameter s in the birth pulse function

$$\nu(t) = \alpha_0 + ke^{-s\cos^2(\pi t/12 - \varphi)}. \tag{2.9}$$

During this experiment, it is important to ensure that the integral of the birth pulse remains the same as before, which means

$$\int_1^{365} (\alpha_0 + ke^{-s\cos^2(\pi t/12 - \varphi)}), dt = 39.214309. \tag{2.10}$$

This assumption implies that the number of juveniles captured over the year, approximately 39, remains constant even as the capture window changes, with a background birthing rate included so that there are births throughout the year.

Now we can begin experiments, so here we are going to test two different scenarios, which are

— the impact of shifting the seasonal peak of births by varying φ (figure 3) and

— the impact of widening the birthing season by varying s (figure 4),

which are both potential impacts of varying land use and climate and we can estimate the periodic basic reproductive number ($\mathcal{R}_p$) and determine the parameters that the model is sensitive to using a sensitivity analysis.

Downloaded from https://royalsocietypublishing.org/ on 31 July 2024

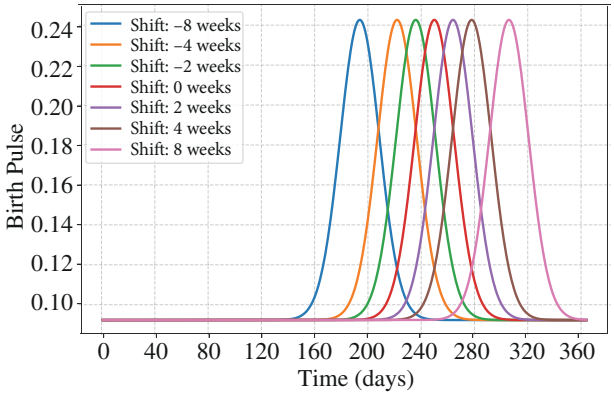

Figure 3. Shifting the seasonal birthing peak.

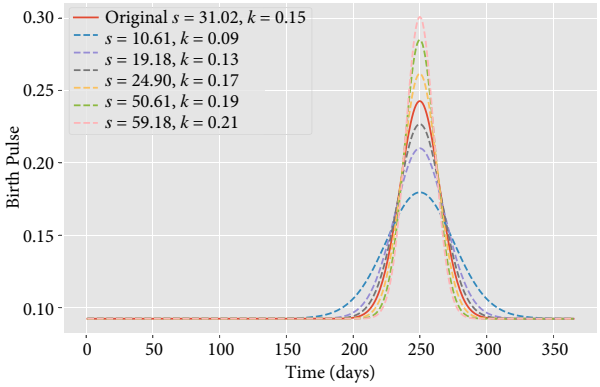

Figure 4. Comparison of the size and synchrony of birth pulses for the original fitted parameters and selected varying parameters with increased or decreased synchrony, but same per capita annual birth rate.

2.2. Time-average basic reproduction number

Two primary approaches used for calculating the basic reproductive number in non-autonomous disease transmission periodic systems are the time-average method and the linear operator method [22,51–54]. Mitchell and Kribs [55] conducted a comparison of the two methods, identifying the conditions under which they align. In this work, we use the time-average method to establish the $\mathcal{R}_p$ of the model (2.1).

When the population is LASV free, we have $I_j = C_j = R_j = I_a = C_a = R_a = 0$, and the model (2.1) has a disease-free equilibrium, denoted ε_0 given by

$$\varepsilon_0 = (S_j^*, I_j^*, C_j^*, R_j^*, S_a^*, I_a^*, C_a^*, R_a^*) = (N_{S_j}, 0,0,0, N_{S_a}, 0,0,0), \tag{2.11}$$

where N_{S_j} and N_{S_a} are the initial susceptible juveniles and adults.

Hence, linearizing system (2.1) at ε_0, we obtain the following equations:

$$\begin{aligned}
\frac{dI_j}{dt} &= (\beta_{ja}I_a + \beta_{jj}I_j + \beta_c(C_j + C_a))S_j^* - \tau_j I_j - \gamma_j I_j - \theta\mu_j I_j\left(\frac{N}{K}\right)\\
\frac{dC_j}{dt} &= \nu(\rho(I_a + C_a)) - \tau_j C_j - \theta\mu_j C_j\left(\frac{N}{K}\right)\\
\frac{dI_a}{dt} &= \tau_j I_j + (\beta_{aa}I_a + \beta_{ja}I_j + \beta_c(C_a + C_j))S_a^* - \gamma_a I_a - \theta\mu_a I_a\left(\frac{N}{K}\right)\\
\frac{dC_a}{dt} &= \tau_j C_j - \theta\mu_a C_a\left(\frac{N}{K}\right).
\end{aligned} \tag{2.12}$$

Using the notation in [56], the next generation matrix F and V associated with the model (2.1) are given, respectively, by

$$F = \begin{pmatrix} \beta_{jj}S_j^* & \beta_c S_j^* & \beta_{ja}S_j^* & \beta_c S_j^* \\ 0 & 0 & 0 & 0 \\ \beta_{ja}S_a^* & \beta_c S_a^* & \beta_{aa}S_a^* & \beta_c S_a^* \\ 0 & 0 & 0 & 0 \end{pmatrix}, \tag{2.13}$$

Downloaded from https://royalsocietypublishing.org/ on 31 July 2024

$$V = \begin{pmatrix} \tau_j + \gamma_j + \theta\mu_j(\frac{N}{K}) & 0 & 0 & 0 \\ 0 & \tau_j + \theta\mu_j(\frac{N}{K}) & -\nu(t)\rho & -\nu(t)\rho \\ -\tau_j & 0 & \gamma_a + \theta\mu_a(\frac{N}{K}) & 0 \\ 0 & -\tau_j & 0 & \theta\mu_a(\frac{N}{K}) \end{pmatrix}. \tag{2.14}$$

$$\begin{aligned} \mathcal{R}_p &= \rho(FV^{-1}) \\ &= \frac{KS_a^*\left(K^2\beta_{aa}\nu(t)\rho\tau_j - K^2\beta_c\nu(t)\rho\tau_j - KN\beta_{aa}\mu_a\tau_j\theta - KN\beta_c\mu_a\nu(t)\rho\theta - N^2\beta_{aa}\mu_a\mu_j\theta^2\right)}{K^3\gamma_a\nu(t)\rho\tau_j - K^2N\gamma_a\mu_a\tau_j\theta + K^2N\mu_a\nu(t)\rho\tau_j\theta - KN^2\gamma_a\mu_a\mu_j\theta^2 - KN^2\mu_a^2\tau_j\theta^2 - N^3\mu_a^2\mu_j\theta^3}, \end{aligned}$$

where $\rho(FV^{-1})$ is the spectral radius of the next generation matrix FV^{-1} at the disease-free equilibrium ε_0.

Replacing $\nu(t)$ by its long-term average [55] we have

$$[\nu] := \frac{1}{\omega}\int_0^{\omega} \nu(t)dt.$$

Then, we have the time-average $\widetilde{\mathcal{R}}_p$ given by

$$\widetilde{\mathcal{R}}_p = \frac{KS_a^*\left(K^2\beta_{aa}[\nu]\rho\tau_j - K^2\beta_c[\nu]\rho\tau_j - KN\beta_{aa}\mu_a\tau_j\theta - KN\beta_c\mu_a[\nu]\rho\theta - N^2\beta_{aa}\mu_a\mu_j\theta^2\right)}{K^3\gamma_a[\nu]\rho\tau_j - K^2N\gamma_a\mu_a\tau_j\theta + K^2N\mu_a[\nu]\rho\tau_j\theta - KN^2\gamma_a\mu_a\mu_j\theta^2 - KN^2\mu_a^2\tau_j\theta^2 - N^3\mu_a^2\mu_j\theta^3}. \tag{2.15}$$

2.3. Sensitivity analysis

In this section, we explore the significance of model parameters on transmission dynamics of LASV using sensitivity analysis. The sensitivity analysis enables the assessment of proportional change in the basic reproduction number as the model parameter is varied [57]. For the LASV model (2.1), the normalized forward sensitivity indices of the time-average basic reproduction number $\widetilde{\mathcal{R}}_p$ with respect to the parameter ζ are calculated using the following:

$$\Gamma_{\zeta}^{\widetilde{\mathcal{R}}_p} = \frac{\partial\widetilde{\mathcal{R}}_p}{\partial\zeta} \times \frac{\zeta}{\widetilde{\mathcal{R}}_p}, \tag{2.16}$$

where ζ is any parameter in the expression of $\widetilde{\mathcal{R}}_p$.

We also test the impact of the initial numbers of chronically infected juvenile populations by varying in the initial conditions, shown in the electronic supplementary material, appendix.

3. Results

3.1. Simulation results

Overall, our model replicates some key features of LASV dynamics in *M. natalensis*. There is a peak of births and viral prevalence in a two- to three-month period, correlating to the months of August and September, with the highest viral prevalence occurring in the juvenile class (i.e. approximately 10% of adults and 56% of juveniles infected). The above observation is consistent with the presence and absence of chronically infected individuals in both adults and juveniles.

Viral prevalence and seasonal changes in birthing timing. Iif changes like climate or land use change move the seasonal peak of birthing (e.g. figure 3), our simulation suggests that this will simply shift the peak of viral prevalence. The results of the simulation are shown in figure 5.

Viral prevalence and seasonal changes in birthing synchrony. If changes like climate or land use alter the synchrony of the seasonal birth peak (e.g. figure 4), our simulation suggests that this will alter both the timing and height of the peak viral prevalence, primarily in the juvenile population. The impact of changes in birthing patterns is most pronounced in the number of infected juveniles (I_j), with smaller effects on infected adults (I_a). Adult chronic infection levels (C_a) remain relatively stable across different birth synchrony scenarios. The results of the simulation are shown in figure 6.

The impact of the changes in birthing is largely seen in the juvenile, rather than adult classes, with the adult numbers of infected individuals relatively stable (figures 6 and 3).

The impact of varying the initial numbers of chronically infected juvenile populations in the initial conditions is shown in the electronic supplementary material (appendix figures A1 and A2).

Downloaded from https://royalsocietypublishing.org/ on 31 July 2024

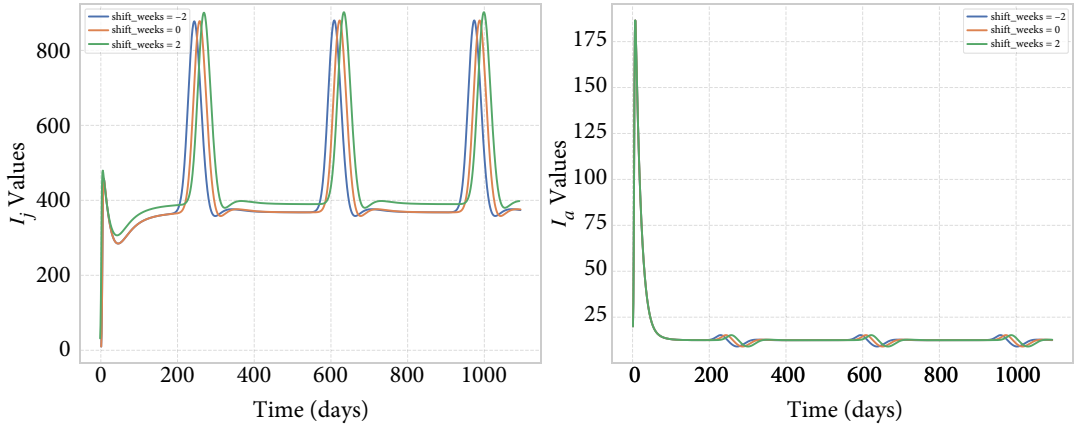

Figure 5. Effect of changing the birth pulse birth timing.

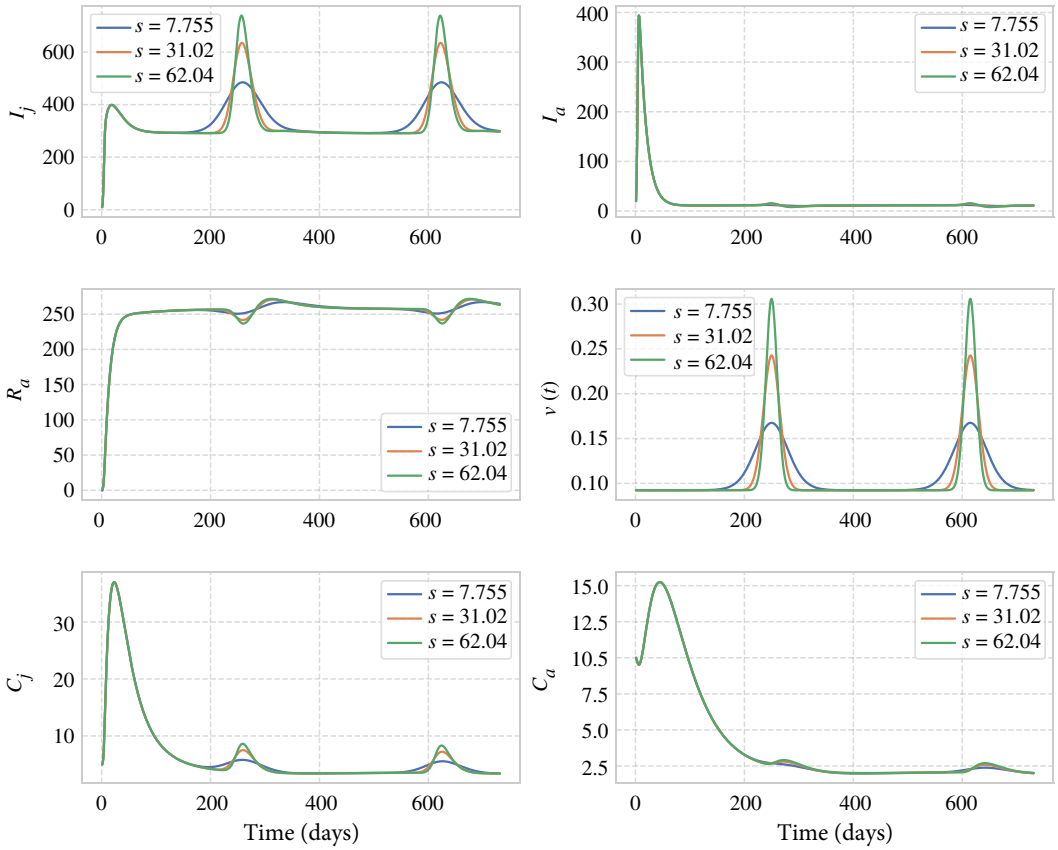

Figure 6. Effect of changing the birth pulse birth width.

3.2. Sensitivity analysis

The sensitivity indices of $\widetilde{\mathcal{R}}_p$ to parameters for the LASV model (2.1), evaluated at the parameter values in table 1, are provided in table 2. The positive sign of the sensitivity index of the time-average basic reproduction number, $\widetilde{\mathcal{R}}_p$, with respect to the model parameters indicates that an increase (or decrease) in the value of each parameter will result in an increase (or decrease) in the basic reproduction number of the disease. It is observed from table 2 that four parameters, K, β_{aa}, μ_a and θ, have the greatest impact on $\widetilde{\mathcal{R}}_p$, with a fifth, γ_a, also contributing. The plot of the sensitivity indices for each parameter in $\widetilde{\mathcal{R}}_p$ is shown in figure 7. The positive indices of parameters K and β_{aa} show that they have a direct relation with $\widetilde{\mathcal{R}}_p$. For example, an increase or decrease in the value of K by 10% would increase or decrease the value of $\widetilde{\mathcal{R}}_p$ by 8.22%. The negative indices of parameters μ_a and γ_a show that they have an inverse relation with $\widetilde{\mathcal{R}}_p$. Increasing the value of μ_a by 10% would results in 8.22% decrease in the value of $\widetilde{\mathcal{R}}_p$.

The results of this sensitivity analysis can be seen in simulations. For example, figure 8 shows the impact of varying μ_a and μ_j on I_j.

Downloaded from https://royalsocietypublishing.org/ on 31 July 2024

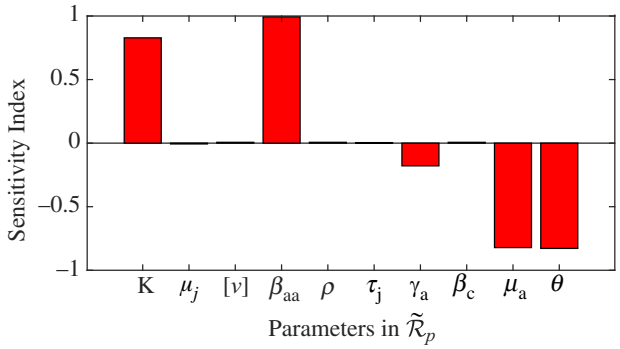

Figure 7. Sensitivity indices of the time-average basic reproduction number $\widetilde{\mathcal{R}}_p$.

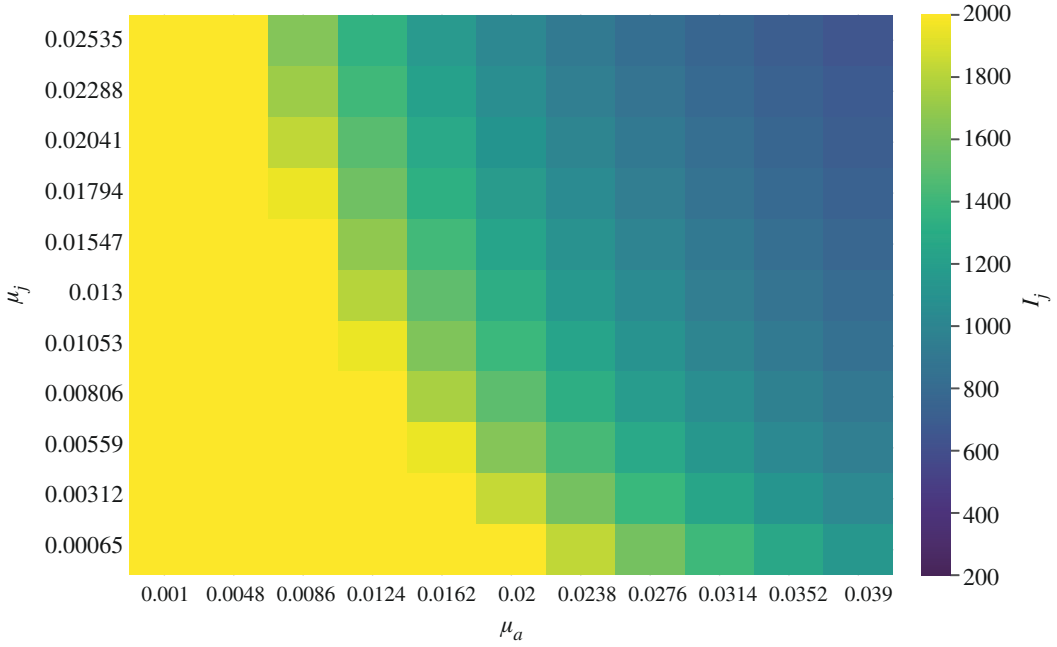

Figure 8. The influence of varying μ_a and μ_j on I_j on day 258 of simulations is examined. We have selected a range of 95 variations on either side of the observed values of $\mu_j = 0.013$ and $\mu_a = 0.02$ to explore extreme scenarios or situations characterized by high uncertainty surrounding the observed values of μ_a and μ_j.

4. Discussion

We developed a *SICR* model of LASV dynamics in its rodent host, *M. natalensis*. Our simulations suggest that altering rodent dynamics, such as through changing resource availability with climate or land use change, will impact LASV dynamics in two ways. First, by shifting the peak of viral prevalence if seasonality changes, thus impacting the potential risk of LASV in people. Second, by modelling the impacts of shifting synchrony. We note that the infection prevalence is very stable in adults, and the impacts are largely seen among juveniles, potentially helping inform risk mitigation strategies.

Our sensitivity analyses suggest there are four key parameters that impact $\widetilde{\mathcal{R}}_p$: carrying capacity ($K$), adult mortality ($\mu_a$), adult-to-adult transmission rate (β_{aa}) and additional disease-induced mortality (ω). Impacting these will probably have the greatest changes on LASV dynamics. A fifth parameter, γ_a, the infection recovery rate, also has greater impact on $\widetilde{\mathcal{R}}_p$, than the remaining parameters. Notably, carrying capacity and adult mortality are two parameters that can probably be substantially impacted by humans, because, for example, crops might provide resources for *M. natalensis* [25,28] and increase or decrease mortality, along with human activities such as rodent control and killing [17]. Changes in density will also probably impact β_{aa}, which itself is dependent on contact rates [58,59]. These responses are probably general too, i.e. in North American deer mouse, *Peromyscus maniculatus*, a reservoir host for numerous zoonotic pathogens common in peridomestic settings, contact rates have been shown to significantly increase in response to feeding [60].

Our findings have similarities and differences to other systems. Our sensitivity analyses are not directly comparable to sensitivity analyses for other recent LASV model with time-dependent parameters that have different model structures and include human transmission [16,22]. However, Ibrahim & Dénes [22] found both reproduction numbers they modelled, a basic R_0 and time-average basic reproduction number $\widetilde{\mathcal{R}}_p$ increase by increasing the transmission rates and rodent birthing rates, the latter differing from our findings. In other systems, sensitivity analyses of filovirus (e.g. Ebola virus, Marburg virus) dynamics and persistence in bat host populations, viruses which also cause zoonotic VHF and disease in people in Africa, suggest that persistence is significantly positively affected by increasing the incubation period, infectious period and overall birth rate,

Downloaded from https://royalsocietypublishing.org/ on 31 July 2024

Table 2. Sensitivity indices of the time-average basic reproduction number with respect to parameters for the LASV model (2.1).

parameter	index	increase or decrease (%)	impact on $\widetilde{\mathcal{R}}_p$
K	+0.8282	10	8.22%
μ_j	−0.006452	10	0.065%
$[\nu]$	+0.00652	10	0.065%
β_{aa}	+0.9935	10	9.94%
ρ	+0.00652	10	0.065%
τ_j	+0.000415	10	0.0042%
γ_a	−0.1787	10	1.78%
β_c	+0.00651	10	0.065%
μ_a	−0.8218	10	8.22%
θ	−0.8282	10	8.28%

and negatively by increasing synchrony of the birth pulse, rather than carrying capacity or mortality rates [61], suggesting that processes that affect different parameters will probably alter the risk of infection transmission among emerging viruses differently.

Our sensitivity analyses also help us understand which parameters might be important to measure in the field [62]; we used some data from East African *M. natalensis* populations to model LASV, a disease occurring in West Africa, because of a lack of appropriate data. Despite this, our work and that of others suggest in West Africa the *M. natalensis* population dynamic fluctuation depends on seasonally available food, and human activities, habitat or rainfall changes will probably impact these. These studies are important; in Upper Guinea a seven-year rodent control experiment with 10–30 day control periods annually and a single intensive three-month trapping exercise led to a rapid increase in rodents following control efforts with concurrently high LASV infection rates, suggesting density-dependent compensation drove increased viral incidence [17]. Our model supports these field studies, suggesting continuous control to reduce the carrying capacity (K) and adult mortality (μ_a) might be most successful in reducing $\widetilde{\mathcal{R}}_p$. Figure 8 shows the relative impact of increasing mortality on the infected juvenile classes (I_j), which have greater prevalence than adults.

We aimed to have a parsimonious, but biologically realistic model that allows us to run the experiments we wanted. We limited our simulations to those models with seasonal forcing, because without seasonal forcing we would expect dampening oscillating dynamics until an endemic state is produced and then risk to humans is owing to seasonally changing contact rates (if they exist) and human behaviours and risk factors, such as immunity. This would be true even in the presence of other dynamic factors, such as maternal antibody, in a deterministic model. We have previously looked at the impact of maternally derived antibodies in other systems, including those with strong seasonality (e.g. [63,64]). In LASV–*M. natalensis* system, it appears that maternally derived antibodies last about 30 days on average. On the whole, including maternally derived antibodies is likely to simply dampen the seasonality due to seasonal forcing due to birthing, thus having an analogous role to decreasing the birthing synchrony which we model.

Future analyses. We used a relatively simple model; however, additional details could be added to future models and questions asked. Furthermore, our model is deterministic. LASV is maintained in *M. natalensis* populations, therefore this suffices; however, a stochastic version of this model would help to explore how infection may or may not fade out, with alternative questions, such as below, through stochastic simulations [43,61,65].

There are multiple questions that we did not ask. These include:

- How might an incubation period, or exposed (E) class, alter transmission dynamics? There is evidence of a short incubation period for LASV in *M. natalensis*; peak viral RNA was detected in nine tissues (all tested) of experimentally infected mice just days 7 and 14 post-infection [37], so animals are probably infected just days into infection. However, longer incubation periods may alter the dynamics. This may be more important for viral maintenance in the populations in systems with very highly synchronized birthing, as observed in some bat systems [61,64] or, conversely, where there is little seasonality, such in Niamey, Niger, in the Sahel, where *M. natalensis* is mostly associated with people, living mostly indoors [50], because incubation periods may allow a greater probability of viral persistence in a population [61].
- How does vertical transmission of LASV in juvenile rodents impact overall virus prevalence and persistence in the population? The model could examine different rates of (pseudo)vertical transmission, which might facilitate persistence and be important for resurgence of infections following large declines in populations, including following control [17].
- What is the impact of seasonal fluctuations in host population density on LASV transmission dynamics? The model could explore different scenarios with high versus low amplitude population cycles. New datasets for *M. natalensis*, such as a recent 29-year dataset in East Africa, will allow more data-driven analyses to be performed [46] to understand time-varying risk in more detail. Climate change is predicted to impact West Africa in two alternative, but plausible ways, with either decreased rainfall projected in the Gulf of Guinea in spring and the Sahel in summer, or increased summer rainfall over both regions [31]. In years when rainfall was below average and the wet season was short, *M. natalensis* population densities were significantly lower [24]. Moreover, these could also incorporate aspects of control to better

Downloaded from https://royalsocietypublishing.org/ on 31 July 2024

understand how different control measures might dampen or even increase the viral incidence in populations, as seen in Guinea, West Africa [17].

- What is the effect of rodent reproductive seasonality and birth pulses on LASV prevalence over time? Related to the three questions above, the model could test shifting or expanding/contracting birth pulse seasons that change through time with varying amplitudes.
- How does acquired immunity following LASV infection in rodents impact transmission dynamics and prevalence? As discussed above, the model could incorporate waning immunity and reinfection of recovered individuals and maternally derived antibodies in the young, as in Mariën *et al*. [23].
- How sensitive are the model predictions to uncertainties in key parameters not included or included in other terms, such as contact rates and transmission probabilities within β terms? A sensitivity analysis of a more complex model could identify critical knowledge gaps, along with stochastic models to help understand viral persistence. Common findings across models with different structures strengthen the case for these parameters being important drivers of viral persistence.
- Can the model be expanded to connect LASV dynamics in rodents to human exposure risk? Adding a human component, such as seasonally changing behaviours (and so exposures) could better predict case and outbreak risk [13,21]. Efforts have been made (e.g. [16,22]), but as better data become available, models can help identify key transmission dynamics between and among hosts [9,66].
- How would interventions like rodent control or landscape modification potentially impact LASV transmission in rodent populations and human risk? Adding intervention effects could inform disease control, beyond our findings that carrying capacity (K) and adult mortality (μ_a) are key parameters for this system.
- How might new species recently identified as potential hosts impact the viral dynamics and human risk? Recent studies such as [1,3] have identified other rodent species that can be infected with LASV. These are typically even less well studied than *M. natalensis* in West Africa, but future models could include differing host dynamics to better understand if and how these alternative hosts might alter viral persistence and human risk.

Future analyses can use our model to inform field and experimental studies [62], with temporally and spatially varying data particularly useful to further validate the model predictions. Recent analyses with a similar *SEIR*-based model, including the same periodically forced seasonal birthing from [48] and an approximate Bayesian computation scheme to fit the model to the case data from 2018 to 2020 in Nigeria, also showed that the dynamics of the rodent reservoir probably lead to periodic increases in spillover risk [16], but this lacked the rodent data and so further work is needed. Our analyses help determine which parameters of the models outcomes are sensitive to, and so which aspects of the system will lead to changing risk and require better data.

In summary, we developed an *SIR*-based model of LASV dynamics in its rodent host, *Mastomys natalensis*, with a persistently infected class and seasonal birthing to test how climate and land use changes that impact birthing might alter viral dynamics and, therefore, risk. Our simulations suggest viral dynamics in adults is mainly stable, with greater variation in the young, with likely predictable shifts in rodent birthing timing and synchrony corresponding to viral prevalence shifts. Our $\widetilde{\mathcal{R}}_p$ calculation using a time-average method and with a sensitivity analysis show carrying capacity (K), the transmission parameter among adults (β_{aa}) and adult mortality (μ_a) are key parameters impacting LASV in $\widetilde{\mathcal{R}}_p$ *M. natalensis* most, all of which are impacted by directly and indirectly human activities and interventions.

Ethics. This work did not require ethical approval from a human subject or animal welfare committee.

Data accessibility. All code and data are available at Zenodo [67].

Supplementary material is available online [68].

Declaration of AI use. We have not used AI-assisted technologies in creating this article.

Authors' contributions. R.S.J.: formal analysis, investigation, methodology, visualization, writing—original draft, writing—review and editing; H.O.F.: formal analysis, investigation, methodology, visualization, writing—original draft, writing—review and editing; D.T.S.H.: conceptualization, investigation, methodology, validation, writing—original draft, writing—review and editing.

All authors gave final approval for publication and agreed to be held accountable for the work performed therein.

Conflict of interest declaration. We declare we have no competing interests.

Funding. This work was supported by funds from the Royal Society Te Apārangi Rutherford Discovery Fellowship (RDF-MAU1701, D.T.S.H.), Bryce Carmine and Anne Carmine (née Percival) through the Massey University Foundation (D.T.S.H., R.S.M.) and the Percival Carmine Chair in Epidemiology and Public Health (D.T.S.H.). R.S.J acknowledges the financial support provided by Te Pūnaha Matatini. The funders played no role in the design of the study, the decision to publish, or the preparation of the manuscript.

Acknowledgements. We thank the reviewers for their comments and our funders for their support.

References

1. Kenmoe S *et al*. 2020 Systematic review and meta-analysis of the epidemiology of Lassa virus in humans, rodents and other mammals in sub-Saharan Africa. *PLoS Negl. Trop. Dis.* **14**, e0008589. (doi:10.1371/journal.pntd.0008589)
2. Yaro CA, Kogi E, Opara KN, Batiha GES, Baty RS, Albrakati A, Altalbawy FMA, Etuh IU, Oni JP. 2021 Infection pattern, case fatality rate and spread of Lassa virus in Nigeria. *BMC Infect. Dis.* **21**, 149. (doi:10.1186/s12879-021-05837-x)
3. Bangura U *et al*. 2024 Spatio-temporal spread of Lassa virus and a new rodent host in the Mano River Union area, West Africa. *Emerg. Microbes Infect.* **13**, 2290834. (doi:10.1080/22221751.2023.2290834)

Downloaded from https://royalsocietypublishing.org/ on 31 July 2024

4. Fichet-Calvet E *et al*. 2007 Fluctuation of abundance and Lassa virus prevalence in *Mastomys natalensis* in Guinea, West Africa. *Vector Borne Zoonotic Dis.* **7**, 119–128. (doi:10.1089/vbz.2006.0520)
5. Demby AH *et al*. 2001 Lassa fever in Guinea: II. Distribution and prevalence of Lassa virus infection in small mammals. *Vector Borne Zoonotic Dis.* **1**, 283–297. (doi:10.1089/15303660160025912)
6. Ter Meulen J *et al*. 1996 Hunting of peridomestic rodents and consumption of their meat as possible risk factors for rodent-to-human transmission of Lassa virus in the Republic of Guinea. *Am. J. Trop. Med. Hyg.* **55**, 661–666. (doi:10.4269/ajtmh.1996.55.661)
7. Kafetzopoulou LE *et al*. 2019 Metagenomic sequencing at the epicenter of the Nigeria 2018 Lassa fever outbreak. *Science* **363**, 74–77. (doi:10.1126/science.aau9343)
8. Siddle KJ *et al*. 2018 Genomic analysis of Lassa virus during an increase in cases in Nigeria in 2018. *N. Engl. J. Med.* **379**, 1745–1753. (doi:10.1056/NEJMoa1804498)
9. Lo Iacono G *et al*. 2015 Using modelling to disentangle the relative contributions of zoonotic and anthroponotic transmission: the case of Lassa fever. *PLoS Negl. Trop. Dis.* **9**, e3398. (doi:10.1371/journal.pntd.0003398)
10. Tschismarov R *et al*. 2023 Immunogenicity, safety, and tolerability of a recombinant measles-vectored Lassa fever vaccine: a randomised, placebo-controlled, first-in-human trial. *Lancet.* **401**, 1267–1276. (doi:10.1016/S0140-6736(23)00048-X)
11. Olayemi A *et al*. 2016 Arenavirus diversity and phylogeography of *Mastomys natalensis* rodents, Nigeria. *Emerg. Infect. Dis.* **22**, 694–697. (doi:10.3201/eid2204.150155)
12. Gryseels S, Baird SJE, Borremans B, Makundi R, Leirs H, Goüy de Bellocq J. 2017 When viruses don't go viral: the importance of host phylogeographic structure in the spatial spread of arenaviruses. *PLoS Pathog.* **13**, e1006073. (doi:10.1371/journal.ppat.1006073)
13. Akhmetzhanov AR, Asai Y, Nishiura H. 2019 Quantifying the seasonal drivers of transmission for Lassa fever in Nigeria. *Phil. Trans. R. Soc. B* **374**, 20180268. (doi:10.1098/rstb.2018.0268)
14. Fichet-Calvet E, Lecompte E, Koivogui L, Daffis S, ter Meulen J. 2008 Reproductive characteristics of *Mastomys natalensis* and Lassa virus prevalence in Guinea, West Africa. *Vector Borne Zoonotic Dis.* **8**, 41–48. (doi:10.1089/vbz.2007.0118)
15. Happi AN *et al*. 2022 Increased prevalence of Lassa fever virus-positive rodents and diversity of infected species found during human Lassa fever epidemics in Nigeria. *Microbiol. Spectr.* **10**, e0036622. (doi:10.1128/spectrum.00366-22)
16. McKendrick JQ, Tennant WSD, Tildesley MJ. 2023 Modelling seasonality of Lassa fever incidences and vector dynamics in Nigeria. *PLoS Negl. Trop. Dis.* **17**, e0011543. (doi:10.1371/journal.pntd.0011543)
17. Mariën J *et al*. 2024 Rodent control strategies and Lassa virus: some unexpected effects in Guinea, West Africa. *Emerg. Microbes Infect.* **13**, 2341141. (doi:10.1080/22221751.2024.2341141)
18. Amman BR *et al*. 2014 Marburgvirus resurgence in Kitaka mine bat population after extermination attempts, Uganda. *Emerging Infect. Dis.* **20**, 1761–1764. (doi:10.3201/eid2010.140696)
19. Redding DW, Moses LM, Cunningham AA, Wood J, Jones KE. 2016 Environmental-mechanistic modelling of the impact of global change on human zoonotic disease emergence: a case study of Lassa fever. *Methods Ecol. Evol.* **7**, 646–655. (doi:10.1111/2041-210X.12549)
20. Klitting R *et al*. 2022 Predicting the evolution of the Lassa virus endemic area and population at risk over the next decades. *Nat. Commun.* **13**, 5596. (doi:10.1038/s41467-022-33112-3)
21. Barua S, Dénes A, Ibrahim MA. 2021 A seasonal model to assess intervention strategies for preventing periodic recurrence of Lassa fever. *Heliyon* **7**, e07760. (doi:10.1016/j.heliyon.2021.e07760)
22. Ibrahim MA, Dénes A. 2021 A mathematical model for Lassa fever transmission dynamics in a seasonal environment with a view to the 2017–20 epidemic in Nigeria. *Nonlinear Anal. Real World Appl.* **60**, 103310. (doi:10.1016/j.nonrwa.2021.103310)
23. Mariën J, Borremans B, Kourouma F, Baforday J, Rieger T, Günther S, Magassouba N, Leirs H, Fichet-Calvet E. 2019 Evaluation of rodent control to fight Lassa fever based on field data and mathematical modelling. *Emerg. Microbes Infect.* **8**, 640–649. (doi:10.1080/22221751.2019.1605846)
24. Makundi RH, Massawe AW, Mulungu LS. 2007 Reproduction and population dynamics of *Mastomys natalensis* Smith, 1834 in an agricultural landscape in the Western Usambara mountains, Tanzania. *Integr. Zool.* **2**, 233–238. (doi:10.1111/j.1749-4877.2007.00063.x)
25. Mulungu LS *et al*. 2011 Dietary differences of the multimammate mouse, *Mastomys natalensis* (Smith, 1834), across different habitats and seasons in Tanzania and Swaziland. *Wildl. Res.* **38**, 640. (doi:10.1071/WR11028)
26. Mulungu LS, Ngowo V, Mdangi M, Katakweba AS, Tesha P, Mrosso FP, Mchomvu M, Sheyo PM, Kilonzo BS. 2013 Population dynamics and breeding patterns of multimammate mouse, *Mastomys natalensis* (Smith 1834), in irrigated rice fields in Eastern Tanzania. *Pest Manag. Sci.* **69**, 371–377. (doi:10.1002/ps.3346)
27. Borremans B, Hughes NK, Reijniers J, Sluydts V, Katakweba AAS, Mulungu LS, Sabuni CA, Makundi RH, Leirs H. 2014 Happily together forever: temporal variation in spatial patterns and complete lack of territoriality in a promiscuous rodent. *Pop. Ecol.* **56**, 109–118. (doi:10.1007/s10144-013-0393-2)
28. Mlyashimbi ECM *et al*. 2018 Relationships between seasonal changes in diet of multimammate rat (*Mastomys natalensis*) and its breeding patterns in semi-arid areas in Tanzania. *Cogent Food Agric.* **4**, 1507509. (doi:10.1080/23311932.2018.1507509)
29. Odhiambo RO, Makundi RH, Leirs H, Verhagen R. 2008 Dietary selection in *Mastomys natalensis* (Rodentia: Muridae) in the maize agro-ecosystems of central and Southwestern Tanzania. *Mammalia* **72**, 169–177. (doi:10.1515/MAMM.2008.007)
30. Wilkinson DA, Marshall JC, French NP, Hayman DTS. 2018 Habitat fragmentation, biodiversity loss and the risk of novel infectious disease emergence. *J. R. Soc. Interface* **15**, 20180403. (doi:10.1098/rsif.2018.0403)
31. Dosio A, Turner AG, Tamoffo AT, Sylla MB, Lennard C, Jones RG, Terray L, Nikulin G, Hewitson B. 2020 A tale of two futures: contrasting scenarios of future precipitation for West Africa from an ensemble of regional climate models. *Environ. Res. Lett.* **15**, 064007. (doi:10.1088/1748-9326/ab7fde)
32. Mariën J *et al*. 2020 Density dependence and persistence of Morogoro arenavirus transmission in a fluctuating population of its reservoir host. *J. Anim. Ecol.* **89**, 506–518. (doi:10.1111/1365-2656.13107)
33. Ojo MM, Goufo EFD. 2022 Modeling, analyzing and simulating the dynamics of Lassa fever in Nigeria. *J. Egypt. Math. Soc.* **30**, 1. (doi:10.1186/s42787-022-00138-x)
34. Mariën J *et al*. 2018 Arenavirus infection correlates with lower survival of its natural rodent host in a long-term capture-mark-recapture study. *Parasit. Vectors* **11**, 90. (doi:10.1186/s13071-018-2674-2)
35. Nuismer SL *et al*. 2020 Bayesian estimation of Lassa virus epidemiological parameters: implications for spillover prevention using wildlife vaccination. *PLoS Negl. Trop. Dis.* **14**, e0007920. (doi:10.1371/journal.pntd.0007920)
36. Jones KE *et al*. 2009 PanTHERIA: a species-level database of life history, ecology, and geography of extant and recently extinct mammals: ecological archives E090-184. *Ecology* **90**, 2648–2648. (doi:10.1890/08-1494.1)

Downloaded from https://royalsocietypublishing.org/ on 31 July 2024

37. Safronetz D *et al*. 2022 Temporal analysis of Lassa virus infection and transmission in experimentally infected *Mastomys natalensis*. *PNAS Nexus* **1**, pgac114. (doi:10.1093/pnasnexus/pgac114)
38. Wozniak DM *et al*. 2021 Inoculation route-dependent Lassa virus dissemination and shedding dynamics in the natural reservoir – *Mastomys natalensis*. *Emerg. Microbes Infect.* **10**, 2313–2325. (doi:10.1080/22221751.2021.2008773)
39. Fichet-Calvet E, Becker-Ziaja B, Koivogui L, Günther S. 2014 Lassa serology in natural populations of rodents and horizontal transmission. *Vector Borne Zoonotic Dis.* **14**, 665–674. (doi:10.1089/vbz.2013.1484)
40. Borremans B, Vossen R, Becker-Ziaja B, Gryseels S, Hughes N, Van Gestel M, Van Houtte N, Günther S, Leirs H. 2015 Shedding dynamics of Morogoro virus, an African arenavirus closely related to Lassa virus, in its natural reservoir host *Mastomys natalensis*. *Sci. Rep.* **5**, 10445. (doi:10.1038/srep10445)
41. Borremans B, Leirs H, Gryseels S, Günther S, Makundi R, de Bellocq JG. 2011 Presence of Mopeia virus, an African arenavirus, related to biotope and individual rodent host characteristics: implications for virus transmission. *Vector Borne Zoonotic Dis.* **11**, 1125–1131. (doi:10.1089/vbz.2010.0010)
42. Mariën J *et al*. 2017 No measurable adverse effects of Lassa, Morogoro and Gairo arenaviruses on their rodent reservoir host in natural conditions. *Parasit. Vectors* **10**, 210. (doi:10.1186/s13071-017-2146-0)
43. Hayman DTS, Sam John R, Rohani P. 2022 Transmission models indicate Ebola virus persistence in non-human primate populations is unlikely. *J. R. Soc. Interface* **19**, 20210638. (doi:10.1098/rsif.2021.0638)
44. Hixon MA. 2008 Carrying capacity. In *Encyclopedia of ecology* (eds SE Jørgensen, BD Fath), pp. 528–530. Oxford, UK: Academic Press.
45. Hánová A, Konečný A, Mikula O, Bryjová A, Šumbera R, Bryja J. 2021 Diversity, distribution, and evolutionary history of the most studied African rodents, multimammate mice of the genus *Mastomys*: an overview after a quarter of century of using DNA sequencing. *J. Zool. Syst. Evol. Res.* **59**, 2500–2518. (doi:10.1111/jzs.12569)
46. Leirs H *et al*. 2023 Twenty-nine years of continuous monthly capture-mark-recapture data of multimammate mice (*Mastomys natalensis*) in Morogoro, Tanzania. *Sci. Data* **10**, 798. (doi:10.1038/s41597-023-02700-3)
47. Rohatgi A. 2024 *WebPlotDigitizer*. See https://automeris.io/WebPlotDigitizer.html.
48. Peel AJ, Pulliam JRC, Luis AD, Plowright RK, O'Shea TJ, Hayman DTS, Wood JLN, Webb CT, Restif O. 2014 The effect of seasonal birth pulses on pathogen persistence in wild mammal populations. *Proc. R. Soc. B* **281**, 20132962. (doi:10.1098/rspb.2013.2962)
49. Safronetz D *et al*. 2021 Establishment of a genetically confirmed breeding colony of *Mastomys natalensis* from wild-caught founders from West Africa. *Viruses* **13**, 590. (doi:10.3390/v13040590)
50. Garba M, Dobigny G. 2014 Reproduction in urban commensal rodents: the case of *Mastomys natalensis* from Niamey, Niger. *Mammalia* **78**, 185–189. (doi:10.1515/mammalia-2013-0042)
51. Bacaër N, Guernaoui S. 2006 The epidemic threshold of vector-borne diseases with seasonality. *J. Math. Biol.* **53**, 421–436. (doi:10.1007/s00285-006-0015-0)
52. Wang W, Zhao XQ. 2008 Threshold dynamics for compartmental epidemic models in periodic environments. *J. Dyn. Diff. Equat.* **20**, 699–717. (doi:10.1007/s10884-008-9111-8)
53. Posny D, Wang J. 2014 Computing the basic reproductive numbers for epidemiological models in nonhomogeneous environments. *Appl. Math. Comput.* **242**, 473–490. (doi:10.1016/j.amc.2014.05.079)
54. Bakare EA, Are EB, Abolarin OE, Osanyinlusi SA, Ngwu B, Ubaka ON. 2020 Mathematical modelling and analysis of transmission dynamics of Lassa fever. *J. Appl. Math.* **2020**, 1–18. (doi:10.1155/2020/6131708)
55. Mitchell C, Kribs C. 2017 A comparison of methods for calculating the basic reproductive number for periodic epidemic systems. *Bull. Math. Biol.* **79**, 1846–1869. (doi:10.1007/s11538-017-0309-y)
56. Diekmann O, Heesterbeek JAP, Roberts MG. 2010 The construction of next-generation matrices for compartmental epidemic models. *J. R. Soc. Interface* **7**, 873–885. (doi:10.1098/rsif.2009.0386)
57. Abidemi A, Owolabi KM. 2024 Unravelling the dynamics of Lassa fever transmission with nosocomial infections via non-fractional and fractional mathematical models. *Eur. Phys. J. Plus* **139**, 1–30. (doi:10.1140/epjp/s13360-024-04910-z)
58. Lloyd-Smith JO, George D, Pepin KM, Pitzer VE, Pulliam JRC, Dobson AP, Hudson PJ, Grenfell BT. 2009 Epidemic dynamics at the human-animal interface. *Science* **326**, 1362–1367. (doi:10.1126/science.1177345)
59. Begon M, Bennett M, Bowers RG, French NP, Hazel SM, Turner J. 2002 A clarification of transmission terms in host-microparasite models: numbers, densities and areas. *Epidemiol. Infect.* **129**, 147–153. (doi:10.1017/s0950268802007148)
60. Kuenzi AJ, Luis AD. 2023 Food availability leads to more connected contact networks among peridomestic zoonotic reservoir hosts. *R. Soc. Open Sci.* **10**, 230809. (doi:10.1098/rsos.230809)
61. Hayman DTS. 2015 Biannual birth pulses allow filoviruses to persist in bat populations. *Proc. R. Soc. B* **282**, 20142591. (doi:10.1098/rspb.2014.2591)
62. Restif O *et al*. 2012 Model-guided fieldwork: practical guidelines for multidisciplinary research on wildlife ecological and epidemiological dynamics. *Ecol. Lett.* **15**, 1083–1094. (doi:10.1111/j.1461-0248.2012.01836.x)
63. Peel AJ, Baker KS, Hayman DTS, Broder CC, Cunningham AA, Fooks AR, Garnier R, Wood JLN, Restif O. 2018 Support for viral persistence in bats from age-specific serology and models of maternal immunity. *Sci. Rep.* **8**, 3859. (doi:10.1038/s41598-018-22236-6)
64. Hayman DTS *et al*. 2018 Maternal antibody and the maintenance of a lyssavirus in populations of seasonally breeding African bats. *PLoS One* **13**, e0198563. (doi:10.1371/journal.pone.0198563)
65. Lloyd-Smith JO, Cross PC, Briggs CJ, Daugherty M, Getz WM, Latto J, Sanchez MS, Smith AB, Swei A. 2005 Should we expect population thresholds for wildlife disease *Trends Ecol. Evol.* **20**, 511–519. (doi:10.1016/j.tree.2005.07.004)
66. Lo Iacono G *et al*. 2016 A unified framework for the infection dynamics of zoonotic spillover and spread. *PLoS Negl. Trop. Dis.* **10**, e0004957. (doi:10.1371/journal.pntd.0004957)
67. Reju Sam J. 2024 Modelling Lassa virus dynamics: Lassa virus dynamics in West African rodents. Zenodo. See https://doi.org/10.5281/zenodo.11406343.
68. John RS, Fatoyinbo HO, Hayman D. 2024 Supplementary material from: Modelling lassa virus dynamics in west african mastomys natalensis and the impact of human activities. Figshare. (doi:10.6084/m9.figshare.c.7355003)